

# Lawrence Berkeley National Laboratory

## Lawrence Berkeley National Laboratory

### **Title**

The BERkeley Lab Laser Accelerator (BELLA): A 10 GeV Laser Plasma Accelerator

### **Permalink**

<https://escholarship.org/uc/item/0w17c8fn>

### **Author**

Leemans, W.P.

### **Publication Date**

2011-04-04

# The BERkeley Lab Laser Accelerator (BELLA): A 10 GeV Laser Plasma Accelerator

W.P. Leemans<sup>a,b,c</sup>, R. Duarte<sup>a</sup>, E. Esarey<sup>a,b</sup>, S. Fournier<sup>a</sup>, C.G.R. Geddes<sup>a</sup>, D. Lockhart<sup>a</sup>, C.B. Schroeder<sup>a</sup>, C. Toth<sup>a</sup>, J.-L. Vay<sup>a</sup>, S. Zimmermann<sup>a</sup>

<sup>a</sup>Lawrence Berkeley National Laboratory, 1 Cyclotron Road, Berkeley, CA 94720, USA

<sup>b</sup>University of Nevada, Reno, Reno NV 89557

<sup>c</sup>University of California, Berkeley, CA 94720, USA

**Abstract.** An overview is presented of the design of a 10 GeV laser plasma accelerator (LPA) that will be driven by a PW-class laser system and of the BELLA Project, which has as its primary goal to build and install the required Ti:sapphire laser system for the acceleration experiments. The basic design of the 10 GeV stage aims at operation in the quasi-linear regime, where the laser excited wakes are largely sinusoidal and offer the possibility of accelerating both electrons and positrons. Simulations show that a 10 GeV electron beam can be generated in a meter scale plasma channel guided LPA operating at a density of about  $10^{17}$  cm<sup>-3</sup> and powered by laser pulses containing 30-40 J of energy in a 50-200 fs duration pulse, focused to a spotsizes of 50-100 micron. The lay-out of the facility and laser system will be presented as well as the progress on building the facility.

**Keywords:** Laser, plasma, accelerator, electron beam.

**PACS:** 52.38.Kd, 52.65.Rr, 29.20.Ej

## INTRODUCTION

Laser plasma accelerators (LPA) [1] have the potential to drastically cut the cost of doing science with accelerators due to their much reduced size compared to conventional accelerators of the same energy. The primary areas where state-of-the-art accelerators are utilized are the collider based facilities and the accelerator based light sources. Colliders of the future place formidable demands on the accelerators that drive them. The design of the International Linear Collider (ILC), an RF-driven, TeV-scale, electron-positron machine, calls for a luminosity of  $10^{34}$  cm<sup>-2</sup>s<sup>-1</sup> with average e-beam power of order 14 MW. An LPA-based electron-positron collider could be envisioned by coupling many acceleration stages together [2,3]. The building block of such a collider could be a 10-GeV modular stage of which  $\sim 100$  stages would be required to build a 1 TeV linac. Typical light sources generating intense x-ray beams operate at the 1-15 GeV level, with the higher energy electron beams being used at the world's first x-ray free electron laser (FEL) at the LCLS at SLAC, and the lower energy beams typical of synchrotron based facilities.

In recent years, LPAs have made significant progress towards producing high quality beams with ever higher energy. In 2004, three independent groups showed the first demonstration of relatively narrow energy spread electron beams at the  $\sim 100$  MeV level from mm-scale devices [4-6]. In 2006 the first production was shown of GeV electron beams from a 3 cm long plasma channel guided LPA at LBNL [7]. In the 2006 experiments, the laser peak power was of the order of 40 TW and the operating plasma density was a factor of  $\sim 10$  lower but extended over a  $\sim 10$  times longer distance than in the 2004 experiments. Motivated by the success of these experiments, designs were developed at LBNL to achieve 10 GeV electron beams from meter-scale accelerator structures using a PW-class laser system, which led to the formal BELLA project proposal to the Department of Energy, Office of High Energy Physics in 2007. While it could be decades before a laser plasma accelerator can match the capabilities of something like the proposed International Linear Collider—a 25 miles (40 kilometers) long machine that would produce electrons and positrons at extremely high energies (1000 GeV) -- BELLA represents an essential step towards investigating how more powerful accelerators of the future might be more compact. Systems like BELLA

hold the promise of making possible a table-top accelerator with particle energies in the tens of GeV range, which would be compact and cheap enough for even universities and hospitals to have one.

The project phase of BELLA is comprised of the construction and commissioning of a PW-class laser that will support the research aimed at the development of 10 GeV LPA modules. Upon successful completion of BELLA's project phase, the laser system and facility will be used to demonstrate that high quality 10 GeV electron beams can be generated using a laser powered plasma structure that is about 1 meter long. The research supported by BELLA will also investigate fundamental laser-plasma interaction physics that aims at optimizing the coupling efficiency of laser to electron beam energy, controlling both the energy spread and emittance of the electron beams, and staging multiple LPA modules together. The 10 GeV beams could also be used to study beam driven plasma wakefield acceleration, as well as positron production and subsequent acceleration in plasma based accelerators.

Although its main purpose is accelerator research, the development of a compact 10 GeV accelerator has several potential applications. BELLA could be used to build a free-electron laser (FEL) operating in the soft x-ray window that produces few femtosecond radiation pulses that are intrinsically synchronized to laser pulses, to THz radiation pulses or directly to the electron beam. Such a device could be an extraordinarily valuable tool for biologists, chemists, materials scientists, and biomedical researchers, allowing them to observe ultrashort, nanoscale phenomena.

We next discuss the basic design considerations for a BELLA 10 GeV accelerator stage, followed by simulation results from particle-in-cell codes that are capable of modeling the detailed laser-plasma interaction and acceleration processes. We then present a brief overview of the Project status.

## 10 GEV STAGE DESIGN

### Basic Design Considerations

Plasma-based accelerators can sustain electron plasma waves with electric fields on the order of the non-relativistic wavebreaking field  $E_0 = m_e \omega_p / e$ , or  $E_0 [\text{V/cm}] \approx 0.96 n^{1/2} [\text{cm}^{-3}]$ , where  $\omega_p = (4\pi n_0 e^2 / m_e)^{1/2}$  is the electron plasma frequency,  $m_e$  and  $e$  are the electron mass and charge, respectively,  $c$  is the vacuum speed of light and  $n_0$  is the ambient electron density [1]. For example,  $n_0 = 10^{18} \text{ cm}^{-3}$  gives  $E_0 \approx 100 \text{ GV/m}$ , which is approximately three orders of magnitude greater than that obtained in conventional RF linacs. The wavelength of the accelerating plasma wave (wakefield) is on the order of the plasma wavelength  $\lambda_p = 2\pi c / \omega_p$ , or  $\lambda_p [\mu\text{m}] \approx 3.3 \times 10^{10} (n_0 [\text{cm}^{-3}])^{-1/2}$ , e.g.,  $\lambda_p \approx 33 \mu\text{m}$  for  $n_0 = 10^{18} \text{ cm}^{-3}$ . This is very short by conventional RF linac standards, which consequently implies that ultra-short ( $< \lambda_p / c$ ) electron bunches can be generated in plasma-based accelerators. An important parameter in the discussion of ultra-intense laser-plasma interactions is the laser strength parameter  $a_0$ , defined as the peak amplitude of the normalized vector potential of the laser field,  $a = eA / mc^2$ . The laser strength parameter is related to the peak intensity  $I$  and power  $P$  of a linearly polarized, Gaussian laser pulse by  $a_0 \approx 0.85 \times 10^{-9} \lambda [\mu\text{m}]^{1/2} [W/\text{cm}^2]$ , and  $P [\text{GW}] \approx 21.5 (a_0 r_0 / \lambda)^2$ , where  $r_0$  is the laser spot size at focus,  $\lambda = 2\pi / k$  is the laser wavelength,  $\omega = ck$  is the laser frequency,  $I = 2P / \pi r_0^2$ , and a vector potential of the form  $a = a_0 \exp(-r^2 / r_0^2) \cos(kz - \omega t) \mathbf{e}_x$  is assumed.

We consider two broad regimes of operation: quasi-linear and strongly nonlinear. In both regimes, scalings [1] indicate that, assuming a guided laser at fixed intensity, the electron energy gain is limited by dephasing and is proportional to  $n^{-1}$  at a length proportional to  $n^{-3/2}$ , where  $n$  is the plasma density. The energy gain in the quasi-linear regime is given by  $\Delta W_d [\text{GeV}] \approx I [W/\text{cm}^2] / n [\text{cm}^{-3}]$ , where it is assumed that the accelerator length was matched to the dephasing length  $L_d \approx (\omega^2 / \omega_p^2) \lambda_p = (n_c / n) \lambda_p$  for  $a_0 = 1$ . Here  $n_c = 1.74 \times 10^{21} \text{ cm}^{-3}$  is the critical plasma density for a laser operating at  $0.8 \mu\text{m}$ . This regime offers advantages including symmetric acceleration of electrons and positrons and shaping of the fields, while the nonlinear regime offers higher gradients and uniform focusing fields. In the strongly non-linear regime,  $a_0 \gg 1$ , the laser is sufficiently intense to completely expel all plasma electrons from its path and create a bubble-like accelerating structure [8,9]. Inside the bubble, large accelerating gradients are generated with linear transverse focusing forces for electrons. Positrons, however, can only be accelerated and focused over a very narrow region. Furthermore, continuous injection of plasma electrons from the surrounding plasma can occur along the entire length of the accelerator structure, which would result in the generation of electron beams with significant low energy background. Although the BELLA laser system will be able to access both the quasi-linear and strongly non-linear regime, in this paper we will concentrate on the design of a 10 GeV stage in the quasi-linear regime.

There are several important basic design considerations for operation in the quasi-linear regime where the wake is approximately sinusoidal. Linear theory describes the wake and energy gain as being proportional to intensity. The normalized vector potential of the drive laser beam,  $a_0$ , should be of order unity and the laser pulse length is of the order of half the plasma period. This ensures that the wake remains roughly sinusoidal, that the laser pulse couples resonantly to the plasma wave and that the dephasing distance (over which the electron outruns the accelerating wave) and the pump depletion distance (over which the laser depletes its energy by one e-folding) are about equal. The laser power must be near or below the threshold for relativistic self-focusing, as otherwise the laser self-focuses resulting in an intensity increase that can enter the non-linear regime. For  $a_0=1$ , this requires a laser spot not larger than the plasma wavelength  $\lambda_p$  ( $k_p w_0 < 2\pi$ ). On the other hand, guiding of modes with  $k_p w_0 < \pi$  significantly reduces laser group velocity and hence energy gain due to the relatively short dephasing distance. These limits on spot size set the power range for the laser.

The basic design of the 10 GeV LPA accelerating module is based on the assumption of an externally injected beam. Production of the initial electron beam could be accomplished in a preceding LPA of mm-scale (e.g. gas jet based) or cm-scale (capillary discharge based) by relying on the highly non-linear or bubble regime, or use techniques such as down ramp [10,11] or colliding pulse injection [12,13]. In this two-stage design, an injection structure would be integrated with the main, meter-scale, accelerator structure that is designed to operate without self-trapping [14]. This so-called dark current free structure provides the best prospect for generating low energy spread high quality beams by avoiding continuous injection along the entire length of the plasma structure.

As a numerical example of a basic LPA design that can achieve  $\Delta W_d[\text{GeV}] = 10$  GeV in the quasi-linear regime, i.e.,  $a_0 \sim 1$  or  $I = 1.73 \times 10^{18}$  W/cm<sup>2</sup>, we apply the basic scaling laws and constraints discussed above. We find that a  $\sim 40$  J laser operating at 0.8  $\mu\text{m}$  wavelength, with a pulse duration of  $\sim 260$  fs focused to a spot size of  $\sim 60$   $\mu\text{m}$  and a 0.8 m long plasma at  $\sim 1.73 \times 10^{17}$  cm<sup>-3</sup> density are required, where we assumed  $k_p w_0 = 5.9$  and  $P/P_c = 0.9$ .

These simple scaling laws do not include important effects such as laser self-focusing and other non-linear process, and do not model the details of laser beam evolution, nor the effect of the accelerated beam on the plasma wake (i.e., beam loading). More accurate modeling using two dimensional (2D) and three dimensional (3D) simulations have been performed. Due to the fact that 3D-simulations of a meter-scale LPA are computationally very challenging, a limited number of them have been done to date. Fortunately, simulations show that, in the linear regime, 2D simulations reproduce the wake with sufficient accuracy, as well as focusing and other properties of 3D simulations. In addition, a breakthrough in simulating these meter-scale LPAs in full 3D has been achieved through the use of a Lorentz boosted frame [15-17]. These simulations will be discussed next.

## Particle-in-Cell Simulations of a 10 GeV Stage

To capture laser pulse evolution and particle beam effects, an extensive set of simulations has been performed. Several particle-in-cell (PIC) methods have been applied: (1) direct explicit simulations using moving windows and scaling of plasma density, (2) reduced simulation models including envelope simulations and (3) Lorentz boosted frame simulations that are capable of modeling the entire 10 GeV stage with only minor loss of physics. Detailed parameter studies have been published in Ref [18-20].

The primary modeling of LPAs has been done with explicit PIC simulations using codes such as VORPAL [21], OSIRIS [22], VLPL [23], WAKE [24] and others. In such simulations, Maxwell's equations are solved by finite difference on a computational grid. The forces are then interpolated to the macro-particles, time is advanced, and macro-particle currents are interpolated back to the grid for the next field solve. The simulations resolve the laser wavelength and bunch size (the shortest major scales) and macro-particle kinetics, and were used to model recent experiments [11,25]. Resolving the laser wavelength over the propagation distance ( $\sim 10^6$  steps for cm-scale GeV simulations) and wake volume ( $\sim 10^8$  cells in 3D) drives the computational cost, which is of order  $10^6$  hours for cm-scale GeV runs. For 10 GeV simulations, the cost would increase roughly proportional to the plasma volume times the interaction length. With volume  $\sim \lambda_p^3$  (resolving a wake period) and length  $\sim \lambda_p^3$  (dephasing length), the total simulation cost scales as the 6<sup>th</sup> power of the plasma period, or the third power of the electron beam energy and hence explicit simulations would be on the order of a billion processor hours, which is beyond state of the art.

Due to the fact that direct explicit simulations of 10 GeV stages are beyond the state of the art for m-scale plasmas, reduced simulation models have been implemented, including envelope simulations. These simulations decrease the computational cost by resolving the laser envelope but not its fast oscillation. This in turn allows the use of reduced resolution, and quasistatic codes that use the envelope model and further reduce cost by assuming slow evolution. Such codes are faster, but usually perform less well as the laser depletes, spectrally broadens and

wavelength shifts. Such broadening requires increased resolution or other adaptations to resolve the laser oscillation, and reduces the speed advantage. Validation of the assumptions made in these codes for the parameter regimes of interest is hence needed, but the fact that simulations of the same plasma and laser parameters are possible with a 100 to 10000 times savings in CPU time is a significant advantage.

The primary method that we used to simulate 10 GeV stages for BELLA has relied on scaled simulations [18-21]. Although analytic solutions in the nonlinear, self-consistent, multi-dimensional regime are not available, the plasma response scales with density in both the linear and nonlinear regimes. In particular, the following scalings are obtained:

$$\text{Plasma wavelength} = \text{wake scale} = \lambda_p \sim 1/n^{1/2}$$

$$\text{Self focusing} \sim a_0^2 (k_p w_0)^2 \text{ is constant if } w_0 \text{ scaled with } \lambda_p \text{ for fixed } a_0$$

$$\text{Energy gain} \sim \lambda_p^2 \sim (1/n) \text{ for constant } a_0 \text{ and laser pulse length } k_p L_{\text{laser}} = \text{constant}$$

Simulations were conducted with direct explicit PIC at 10x (i.e.,  $10^{18} \text{ cm}^{-3}$ ) and 100x (i.e.,  $10^{19} \text{ cm}^{-3}$ ) scaled densities. Figure 1 shows the results of two scaled simulations of a 10 GeV stage at  $10^{19} \text{ cm}^{-3}$  and  $10^{18} \text{ cm}^{-3}$  density. Whereas the laser pulse evolution shows subtle differences, the shape of the wake and its amplitude, the dephasing and depletion distances, as well as the energy gain all scaled with density as predicted, within 10% accuracy. This allows designing of 10 GeV stages from short, high ne simulations. One dimensional simulations at  $10^{17} \text{ cm}^{-3}$  density further verified scaling to the design density [20].

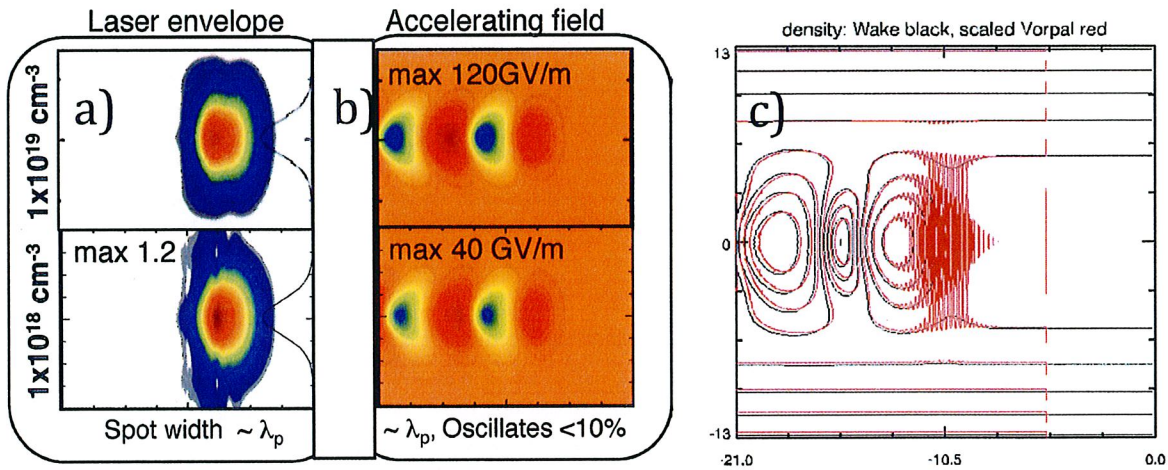


**FIGURE 1.** Scaled simulations of a mildly nonlinear 10 GeV stage using 40 J energy at  $n=10^{17} \text{ cm}^{-3}$ . (a) Laser envelope for  $10^{19} \text{ cm}^{-3}$  (top) and  $10^{18} \text{ cm}^{-3}$  (bottom), (b) accelerating field structure for  $10^{19} \text{ cm}^{-3}$  (top) and  $10^{18} \text{ cm}^{-3}$  (bottom). The wake amplitude, dephasing and depletion distances as well as energy gain scale with density as predicted. (c) Plasma density  $n/n_0$  contours on a fixed scale for (black) WAKE 3D axisymmetric quasistatic PIC simulations at  $10^{17} \text{ cm}^{-3}$  density and (red) VORPAL 2D slab scaled simulations at  $10^{19} \text{ cm}^{-3}$ . The results are nearly indistinguishable from each other except for the fast laser oscillations not modeled in WAKE.

The scaled simulations have been verified by envelope simulations, including simulation of the first 1/3 of a  $k_p L=2$  stage [19]. The scaled simulations in 2D slab geometry were further benchmarked to quasistatic simulations in 3D axisymmetric geometry (r-x, with x the propagation direction and symmetry assumed in theta so that there are two resolved dimensions) at the design density of  $10^{17} \text{ cm}^{-3}$  (see Figure 2). The wake, scaled in units of  $k_p$ , shows agreement at the 1% level across the different numerical models, densities, geometries, and codes. Remaining differences appear to be due to differences in laser pulse shape specification, not fundamental physics. This shows that the scaled simulations are highly valid in this regime.

Simulations were conducted to analyze stage performance with respect to beam loaded gradient and efficiency, by exploring the dependency on the plasma density, the laser amplitude  $a_0$ , width  $k_p w_0$ , and length  $k_p L$ . From linear scalings (where  $a_0$  is constant), it can be found that, for a Gaussian laser pulse, resonant excitation requires a pulse length  $k_p L = 2$ . In principle, at fixed laser energy, a pulse length of zero would excite the largest wake, and self-focusing is also less severe for shorter pulses. To explore the effects of pulse duration, we conducted simulations with constant energy at  $k_p L = 0.5 - 3$  (pulse lengths of 29-170 fs at  $10^{17} \text{ cm}^{-3}$  density). Efficiency and gain were found to be optimal near  $k_p L = 1$ . At this length, approximately 1/3 of the laser is depleted into the wake at

dephasing. The accelerating field was enhanced by 35% relative to the  $k_p L = 2$  case, where only about half as much of the laser is depleted. Scaling of accelerating field was consistent with linear theory. Shorter (longer)  $k_p L$  resulted in depletion before (after) dephasing, both of which reduce efficiency. We are investigating the use of shaped and chirped pulses to further increase depletion and efficiency of an accelerating stage. BELLA will allow studies on the optimum value of  $k_p L$ , and we have already demonstrated use of shaped pulses from a chirped pulse system to enhance coupling [27].

Runs where  $a_0$  or  $w_0$  were increased and  $P/P_c$  was significantly above 1 exhibited self-focusing and did not maintain a quasilinear behavior: for  $k_p L = 2$ ,  $a_0$  cannot be increased much above 1 without decreasing  $k_p w_0$  and, conversely,  $k_p w_0 = 5.3$  is near the maximum that can be used for  $a_0 = 1$ . Runs at  $k_p w_0 < 3$  showed reduced group velocity and also reduced efficiency due to the fact that an increased fraction of the field energy was stored in transverse fields. At  $k_p w_0 \sim 1$ , approximately half of the energy was depleted to transverse fields, and a steep channel density gradient was required to guide the laser spot. This again reduces group velocity and results in undesirable curvature of the wake fronts that affects positron focusing. By design, BELLA will be able to study stages with  $k_p w_0$  from  $\sim 1$  to 6 or more, and with variable  $a_0$ , providing valuable information to the design of optimized stages.

Beam loading studies were conducted in two and three dimensions for a range of beam lengths and widths and showed that approximately 100 pC can be loaded in small radius beams ( $k_p \sigma_r < 1$ ), and 2-500 pC in beams with  $k_p \sigma_r$  of 1-2, where  $\sigma_r$  is the rms electron beam size. The latter corresponds to 10% energy transfer from the laser to the particle beam. Related simulations have shown that greater efficiencies (up to more than 25%) are available by using triangular longitudinal bunch profiles [28,29]. Simulations of self-trapped LPAs indicate that such bunches may be naturally produced in the self-trapping process, and studies are ongoing of coupling these bunches to subsequent accelerator stages and other techniques described below to further increase beam loading efficiency.

An example of input parameters and results of scaled simulations are shown in Table 1. Simulations were done for the high density cases (10x and 100x) and then scaled to the BELLA 10 GeV case. The key parameters ( $a_0$ ,  $k_p L$ ,  $k_p w_0$ ) were optimized while keeping the constraints, discussed above, in mind. The density was set simply by the requirement on the energy gain of the LPA. For comparison, linear dephasing and pump depletion distances are provided. As can be seen, mildly non-linear effects result in stages that are slightly shorter than predicted from linear theory.

**TABLE 1. Example of a design of a Quasilinear 10 GeV BELLA stage and the scaled parameters used for scaled simulations.**

<b>Laser &amp; Plasma Parameters</b>	<b>BELLA 10 GeV</b>	<b>10x density</b>	<b>100x density</b>
Laser Energy [J]	40	1.8	0.04
$a_0$	1.4	1.4	1.4
$\lambda_p$ [ $\mu\text{m}$ ]	107.5	34	10.8
$k_p L_{\text{laser}}$	1	1	1
$L_{\text{laser}}$ [fs]	57	18	5.7
$w_0$ [ $\mu\text{m}$ ]	91.4	28.9	9.1
P [TW]	554	55	5.5
$k_p w_0$	5.3	5.3	5.3
$P/P_c$	1.7	1.7	1.7
Linear Dephasing length [m]	0.97	0.03	0.001
Pump depletion length [m]	1.98	0.06	0.002
Stage length in simulation [m]	0.6	0.0019	0.0006
Energy gain in simulation	10	1	0.1

Techniques to increase the efficiency from laser energy to particle beam energy, and to improve the phase space properties are being developed. Use of density tapering along the propagation length can enhance energy gain and reduce energy spread by allowing phase control in the structure. The difference between laser group velocity in the plasma and electron beam velocity ordinarily results in slippage or dephasing between the electron beam and wake, limiting energy gain and reducing bunch quality because the bunch is subject to fields that vary over propagation. An increasing density gradient causes the plasma wavelength to shorten, and this can be balanced to offset group velocity dephasing, and can be further adjusted to control phase in the wake. Tapered stage designs have been

simulated and indicate that beam energy can be enhanced significantly (3x for a linear taper and ~5x for an optimized taper) and that 10% or greater efficiency with percent energy spread is achievable [18,30].

Methods for controlling and minimizing emittance are also being studied for application in the BELLA 10 GeV stage design. Externally injected bunches loaded into the LPA stage with a radius that is matched to the focusing forces in the stage were shown to be accelerated without significant growth in emittance or bunch size using PIC code simulations, and particle tracking simulations in prescribed fields using the code GPT [31]. These simulations were carried out for parameters based on the analytic design for the 10 GeV stage and used Gaussian transverse laser modes. Although simplest in its implementation, one significant drawback of using Gaussian transverse laser modes, combined with the requirement that, ultimately, the stage must preserve collider-relevant emittances, is the fact that small emittance-matched bunch radii ( $k_p\sigma_r < 0.1$ ) are required. This in turn impacts beam loading performance and stage efficiency. High order transverse modes to shape the accelerating/focusing structure are being explored in order to allow the use of large transverse spots by mixing a zeroth and first order Laguerre-Gaussian mode. Initial simulations show that use of higher order laser modes can decrease focusing forces several fold, allowing use of larger spots and increasing efficiency from laser to accelerated beam while maintaining emittance matching [21,32].

Although density scaled simulations have the advantage over envelope/quasistatic models that they can accurately resolve the wavelength shifting and broadening that occurs as the laser depletes, certain parameters do not scale: the ratio of diffraction range to dephasing, and the electron beam betatron period will differ. Whereas simulating a meter-scale laser-plasma accelerator is not computationally feasible on present machines running direct explicit PIC, a novel technique relying on the use of a Lorentz boosted computational frame has been implemented in WARP3D that allows, for the first time, a full simulation of the BELLA parameters. By recasting the simulation in a frame moving near the speed of light, the technique uses the properties of space-time contraction and dilation offered by special relativity to bridge the disparate space and time scales that exist in the propagation of a micron scale laser wavelength in a meter scale plasma in the laboratory frame [15-17, 20, 33-36]. For a 10 GeV class stage, the maximum attainable speedup is over x10,000 and this was achieved recently for external injection, thanks to advances in the numerical implementation of the technique [36].

Figure 2 shows the density wake excited in the Lorentz boosted frame moving at  $\gamma = 10$  by an intense laser pulse and the externally injected electron beam accelerated by the wake. A 40 J laser pulse with a pulse duration of 67 fs ( $k_pL = 1$ ), was focused to a Gaussian transverse spot size  $w_0 = 89 \mu\text{m}$  at the plasma channel entrance. The plasma channel had an on-axis density  $n_0 = 10^{17} \text{ cm}^{-3}$ , a length of 0.65 m with a parabolic channel (factor=0.6) and a longitudinal taper of the form  $n(x)=n_0(1.32 x+1)$ . Electrons were externally injected with an initial energy of 100 MeV and an initial emittance of 63 mm-mrad. The large input emittance was chosen to maximize the beam radius for efficient beam loading and for emittance matching to the wake's focusing fields [18].

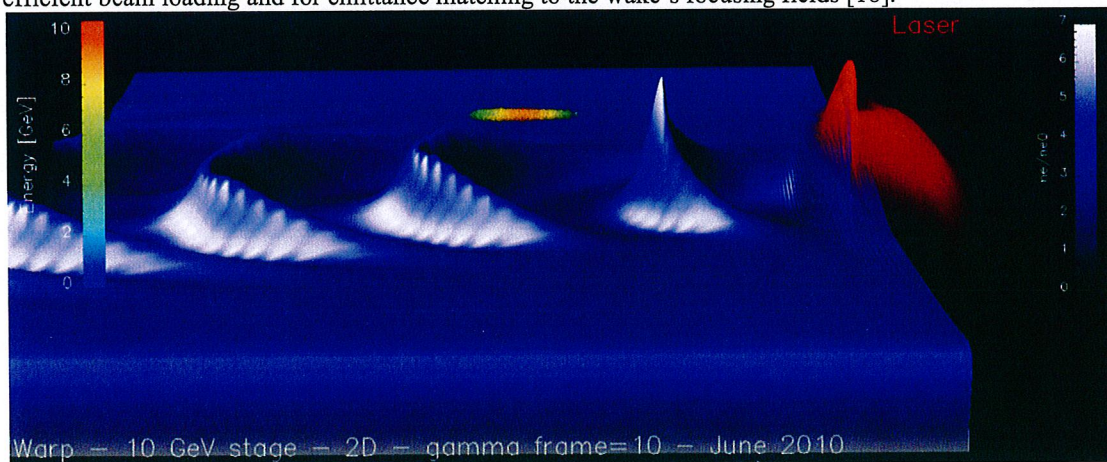


**FIGURE 2.** Simulation result of a 10 GeV LPA stage from the code WARP3D, using a Lorentz boosted frame. The image shows an externally injected electron bunch (rainbow color) riding a density wake (light blue) excited by an intense laser pulse (red), propagating in a 0.65 m long plasma channel. The laser pulse (~40 J in ~67 fs), focused to ~90  $\mu\text{m}$  spot size at the entrance of the channel, has reached the end of the plasma channel. The electron bunch energy has reached up to ~10 GeV.

At the exit of the structure, electrons with energy of up to 9.2 GeV were observed. The color coding indicates the energy reached by the electrons. The depression in the density wake is due to self-consistent beam loading of the injected electron bunch. The time projected energy spread and normalized emittance when exiting the plasma channel were 15% and 57 mm-mrad, respectively. The slice energy spread and emittance of a slice at 9 GeV were 1% and 54 mm-mrad. Whereas this energy spread and emittance is larger than acceptable for collider and light source applications, it has been shown that lower emittance bunches can be accelerated by using high order laser modes to excite the wake and control the transverse focusing forces [32]. Future simulations will aim at optimizing the phase space properties of the bunches including optimization of the taper and the use of higher order laser modes to minimize the emittance.

Although not discussed here, simulations have also been conducted in the nonlinear regime, and show that 10 GeV gain for electrons is also possible using 30-40 J laser pulses, in agreement with published scaling laws [9]. In conclusion, both theoretical modeling and simulations support the fact that 10 GeV electron beams can be produced with a >30 J laser using a pulse length of 50-120 fs and a spot size ranging from 40-100 micron. The acquisition, installation and commissioning of the laser and facility to support the research forms the main scope of the BELLA Project.

## BELLA PROJECT

The scope of the BELLA project includes the design and construction of the conventional facilities required to house and safely operate the BELLA laser (see Figure 3), the acquisition of the BELLA laser system itself, design and construction of ancillary systems to support the laser operations, site and system integration, and performance verification of the BELLA laser system. As shown in Figure 3, the primary elements of the facility include a laser bay which houses the laser system in a temperature and humidity controlled clean room environment (Class 10,000 and local Class 1,000 areas); a power supply and utility room located on top of the roof; a shielded experimental cave; and a control room.

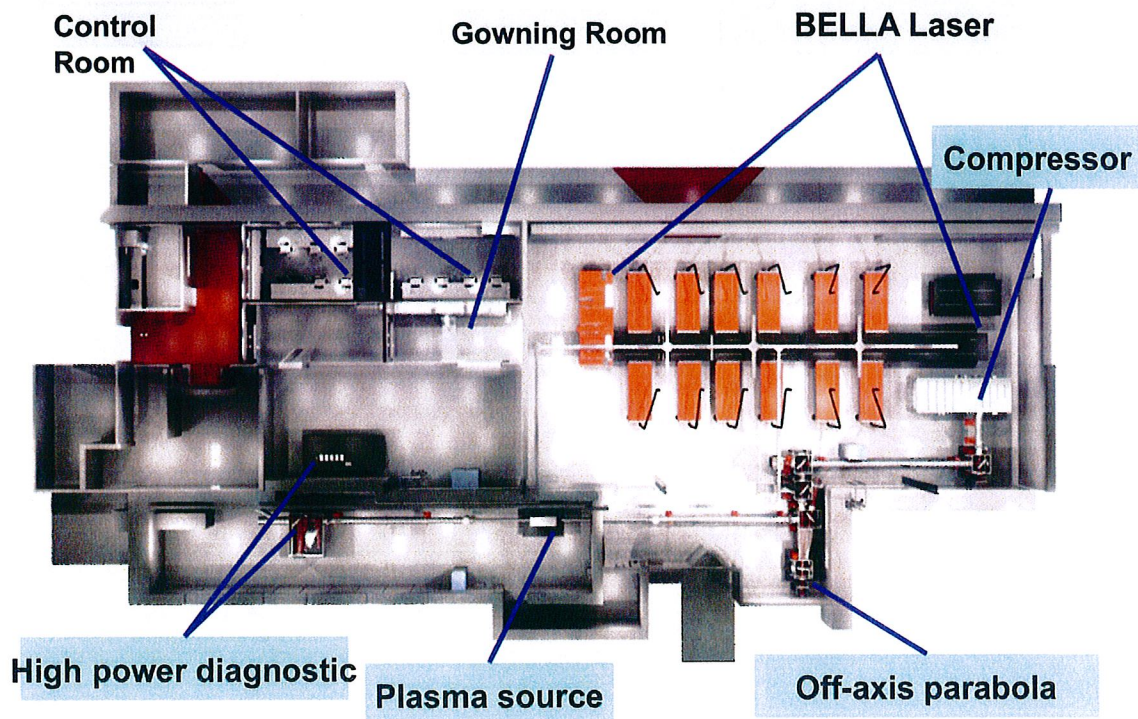


**FIGURE 3.** Lay-out of the BELLA Facility, which is under construction at LBNL.

The BELLA laser is under construction by a commercial vendor (THALES) [37] and will be installed and commissioned at LBNL. The laser system will be capable of delivering >40 Joules of infrared laser energy (at a wavelength  $\sim 0.8 \mu\text{m}$ ) per pulse in <30 fs (i.e., providing >1.3 PW peak optical power in each pulse) for experiments



at a repetition rate of 1 Hz. Based on the design studies for the 10 GeV stage, laser pulses with pulse durations ranging from the minimum pulse duration of 30 fs to several 100 fs long pulses will be provided to the experiment by an adjustable final pulse compressor system. To control the transverse mode profile of the laser beam, a deformable mirror and techniques to produce higher order modes will be implemented.

The laser system will have an elaborate continuous monitoring and diagnostic system, built-in by the vendor, providing vital information on the pulse energies, spectral properties and pointing of the main laser beam at various stages of the laser chain, as well as information on the pump laser beams (homogeneity, amplitude, pointing, timing). A pilot laser beam inserted immediately after the final amplifier will also be part of the system, and will be used for aiming the main laser beam for future experiments.

As part of the BELLA Project phase, there are three subsystems that will control and/or characterize the laser beam after it leaves the laser system. These subsystems are: Compressor to Final Focus Diagnostic system, the Final Focusing and Beam Transport system, and the Final Focus Diagnostic (Low Power). The purpose of the 'Compressor to Final Focus Diagnostic' system situated after the compressor is to measure the key properties of the laser beam prior to sending the pulses onto the final focusing optics. This diagnostic system is being built by THALES and has the capability of monitoring crucial laser parameters of every shot that is sent to the target area, at a 1 Hz repetition rate. The purpose of the 'Final Focus and Beam Transport' system is to focus the beam to a spot size of order 50-100  $\mu\text{m}$  with an achromatic, all-reflective off-axis paraboloidal mirror (OAP). The 'Final Focus Diagnostic (Low Power)' system will be used to verify the laser focal spot quality and its position at a plane where, following completion of the BELLA Project, the plasma based targets will be located during experiments with the BELLA laser.

The BELLA facility has been fully designed to achieve all key performance parameters of the laser system and future experimental systems. This includes clean-room (class 10,000 and 1,000) areas for the laser and experimental areas, with gowning area, assembly area and tightly controlled environmental conditions to minimize temperature and humidity effects as well as low vibration levels; a separate utility room that will house all power supplies and other heat producing equipment; a radiation shielded target area for all high power laser-plasma interaction experiments, including a beam dump to stop and absorb 10 GeV class electron beams; a control room equipped with computer hardware to allow remote operation of the laser system, equipment and personnel safety systems as well as experiments. Facility construction is expected to occur during 2010-2011.

In parallel with the facility construction, work is going on for the design and construction of a 'Final Focus Diagnostic (High Power),' a meter-scale plasma structure, and electron beam diagnostics. The 'Final Focus Diagnostic (High Power)' system will be capable of measuring the beam properties of the laser at all power levels up to full power, at the entrance and exit (1 meter downstream) locations of the plasma target. The entrance of the plasma target will be the vacuum focus location of the BELLA laser beam. The diagnostic includes an all-reflective, achromatic beam attenuation and imaging system, as well a diagnostic suite similar to the post-compressor diagnostic system. Details on the meter-scale structure and electron diagnostic will be discussed in later publications.

## ACKNOWLEDGMENTS

This work was supported by the DOE, Office of High Energy Physics under contract DE-AC02-05CH11231 and greatly benefited from the SciDAC program CompPASS and the resources of NERSC and LBNL cluster Lawrence Livermore. The BELLA Project has received funding from the American Reinvestment and Recovery Act. We would like to thank all present and past LOASIS members and collaborators for their contributions as well as DOE staff from the HEP office and the BSO office. Special thanks go to Ken Barat, Marco Battaglia, David Bruhwiler, John Cary, Estelle Cormier-Michel, Ben Cowan, Jeremy Coyne, Liz Exter, Tony Gonsalves, Steve Gourlay, Bob Gunnion, Jim Krupnick, Nicholas Matlis, Hitoshi Murayama, Jerry O'Hearn, Kem Robinson, George Sanen, Suzanne Suskind, Don Syversrud, Jeroen van Tilborg, Sue Walker-Lam, and Nathan Ybarrolaza for their contributions during different stages of the project. We also want to acknowledge the THALES staff for their contributions.

## REFERENCES

1. E. Esarey, C.B. Schroeder, and W.P. Leemans, *Reviews of Modern Physics* 81, 1229-1285 (2009).
2. W.P. Leemans and E. Esarey, *Physics Today* 62, 44-49 (2009).
3. C.B. Schroeder, E. Esarey, C. Geddes, C. Benedetti and W.P. Leemans, *Phys. Rev. ST-AB*, in print (2010).

4. C. G. R. Geddes et al., Nature 431, 538 (2004).
5. S. P. D. Mangles et al., Nature 431, 535 (2004).
6. J. Faure et al., Nature 431, 541 (2004).
7. W. P. Leemans et al., Nature Physics 2, 696 (2006).
8. A. Pukhov, J. Meyer-ter-Vehn, Appl. Phys. B 74, 355 (2002).
9. W. Lu, C. Huang, M. Zhou, W. B. Mori, and T. Katsouleas, Phys. Rev. Lett. 96, 165002 (2006).
10. S. Bulanov, N. Naumova, F. Pegoraro, and J. Sakai, Phys. Rev. E 58, R5257 (1998).
11. C. G. R. Geddes et al., Phys. Rev. Lett. 100, 215004 (2008).
12. E. Esarey et al., Phys. Rev. Lett. 79, 2682 (1997).
13. J. Faure et al., Nature 444, 737 (2006).
14. A. J. W. Reitsma et al., Phys. Rev. Special Topics Accel. Beams 5, 051302 (2002).
15. J. L. Vay, Phys. Rev. Lett. 98, 130405 (2007).
16. J. L. Vay, et al., J. Phys. Conf. Series 180, 12006 (2009).
17. S. F. Martins et al., Nature Physics 6, 311 (2010).
18. E. Cormier-Michel et al., Proc. 2008 Advanced Accel. Concepts, p. 297 (2009).
19. B. Cowan, D. Bruhwiler, E. Cormier-Michel, E. Esarey, C. G. R. Geddes, P. Messmer and K. Paul, Proc. 2008 Advanced Accel. Concepts Workshop, pp. 307 (2009).
20. G. R. Geddes et al., J. Phys. Conf. Series V 125 pp. 12002/1-11 (2008).
21. C. G. R. Geddes et al., these proceedings.
22. C. Nieter and J. Cary, J. Comp. Phys. 196, 448 (2004).
23. R. G. Hemker et al., Proceedings of the 1999 PAC Conference (1999).
24. A. Pukhov, J. Plasma Phys. 61, 425 (1999).
25. P. Mora and T. M. Antonsen, Phys. Rev. E, vol. 53, pp. 2068 (1996).
26. C. G. R. Geddes et al., Phys. Rev. Lett. 95, 145002 (2005).
27. W. P. Leemans et al., Phys. Rev. Lett. 89, 174802 (2002).
28. T. Katsouleas et al., Part. Accel. 22, 81 (1987).
29. M. Tzoufras et al., Phys. Rev. Lett. 101, 145002 (2008).
30. W. Rittershofer et al., Phys. Plasmas 17, 063104 (2010).
31. <http://www.pulsar.nl/gpt>
32. E. Cormier-Michel et al., Phys. Rev. STAB, submitted.
33. D. L. Bruhwiler, et al., in Proc. 13th Advanced Accelerator Concepts Workshop, Santa Cruz, CA, 2008, p. 29.
34. S. F. Martins, R. A. Fonseca, L. O. Silva, W. Lu, and W. B. Mori, Comput. Phys. Comm. 182, 869-875 (2010).
35. S. F. Martins, et al, these proceedings.
36. J.-L. Vay, et al, these proceedings.
37. <http://thales.nuxit.net/>

#### DISCLAIMER

This document was prepared as an account of work sponsored by the United States Government. While this document is believed to contain correct information, neither the United States Government nor any agency thereof, nor The Regents of the University of California, nor any of their employees, makes any warranty, express or implied, or assumes any legal responsibility for the accuracy, completeness, or usefulness of any information, apparatus, product, or process disclosed, or represents that its use would not infringe privately owned rights. Reference herein to any specific commercial product, process, or service by its trade name, trademark, manufacturer, or otherwise, does not necessarily constitute or imply its endorsement, recommendation, or favoring by the United States Government or any agency thereof, or The Regents of the University of California. The views and opinions of authors expressed herein do not necessarily state or reflect those of the United States Government or any agency thereof or The Regents of the University of California.